ACS Chemical Neuroscience

Letter

Discovery and characterization of 1H-pyrazol-5-yl-2-phenylacetamides as novel, non-urea containing GIRK1/2 potassium channel activators

Joshua M. Wieting, Anish K. Vadukoot, Swagat H. Sharma, Kristopher K. Abney, Thomas M. Bridges, J. Scott Daniels, Ryan D. Morrison, Kevin Wickman, C. David Weaver, and Corey R. Hopkins

ACS Chem. Neurosci., **Just Accepted Manuscript** • DOI: 10.1021/acschemneuro.7b00217 • Publication Date (Web): 11 Jul 2017

Discovery and characterization of 1*H*-pyrazol-5-yl-2-phenylacetamides as novel, non-urea containing GIRK1/2 potassium channel activators

Joshua M. Wieting[†], Anish K. Vadukoot[‡], Swagat Sharma[‡], Kristopher K. Abney[∫], Thomas M. Bridges[∞], J. Scott Daniels[∮], Ryan D. Morrison[∮], Kevin Wickman[∇], C. David Weaver[§,Δ], and Corey R. Hopkins[‡,*]

[†]Vanderbilt Center for Neuroscience Drug Discovery, Vanderbilt University, Nashville, TN 37232, [‡]Department of Pharmaceutical Sciences, College of Pharmacy, University of Nebraska Medical Center, Omaha, NE 68198, [∫]Neuroscience and Pharmacology, Meharry Medical College, Nashville, TN 37208, [∞]Vanderbilt Center for Neuroscience Drug Discovery, Nashville, TN 37232, [∮]Sano Informed Prescribing, Franklin, TN 37067, [∇]Department of Pharmacology, University of Minnesota, Minneapolis, MN 55455, [§]Department of Pharmacology, Vanderbilt University School of Medicine, Nashville, TN 37232, [Δ]Vanderbilt Institute of Chemical Biology, Nashville, TN 37232

Abstract: The G protein regulated inwardly rectifying potassium channels (GIRK, $K_{ir}3$) are a family of inward-rectifying potassium channels, and there is significant evidence supporting the roles of GIRKs in a number of physiological processes and as potential targets for numerous indications. Previously reported urea containing molecules as GIRK1/2 preferring activators have had significant pharmacokinetic liabilities. Here we report a novel series of 1*H*-pyrazolo-5-yl-2-phenylacetamides in an effort to improve upon the PK properties. This series of compounds display nanomolar potency as GIRK1/2 activators with improved brain distribution (rodent $K_p > 0.6$).

KEYWORDS: $K_{ir}3$, GIRK, activator, thallium flux, pharmacokinetics

The G protein-gated regulated inwardly rectifying potassium channels (GIRK, $K_{ir}3$) are a family of inward-rectifying potassium channels and are key effectors in G-protein-coupled receptor cellular signaling pathways.[1] GIRK channels are tetrameric

complexes formed by homo- and heteroassembly among four related subunits (GIRK1-4 or K_{ir}3.1-3.4), which are encoded by the genes *KCNJ3*, *KCNJ6*, *KCNJ9*, and *KCNJ5*, respectively.[2, 3] The GIRK1/2 channel subtype is the most common within the brain, while other subunit combinations have more limited brain distribution; the GIRK1/4 subtype is primarily found in the heart atria, where it plays a key role in regulating heart rate and has been a potential target for the treatment of atrial fibrillation.[4] There is significant evidence supporting the roles of GIRK channels in a number of physiological processes and as potential targets for numerous indications, such as pain perception, epilepsy, reward/addiction and anxiety.[1, 5-7] Unfortunately, due to a dearth of selective pharmacological tool compounds, the roles of GIRK channels as potential therapeutic targets are not well understood. Herein, we report on a new class of GIRK1/2 channel activators with improved pharmacokinetic properties over the previously reported urea-class of activators.

Previous reports of GIRK1/2 channel activators from our laboratory started from a high-throughput screen of the molecular libraries small molecule repository (MLSMR) compound collection – part of the Molecular Libraries Screening Center Network (MLSCN).[8] This screen provided the urea-containing compounds, which led to the discovery of **1** (Figure 1).[9, 10] The urea scaffold has been a rich source of a variety of GIRK1/2 channel activators, as well as 'molecular switches' leading to the mode of pharmacology converting from activator to inhibitor as well as compounds with varying selectivity profiles.[11, 12] Although the urea scaffold has led to the identification of compounds with *in vivo* activity in an antiepileptic model in mice, these compounds suffer from significant pharmacokinetic liabilities, namely poor brain penetration as well

as only modest selectivity against the GIRK1/4 channel subtype.[9, 10] In addition to the urea scaffold, an alternative amide-containing scaffold was reported that resulted from the same MLSCN HTS that yielded the urea scaffold.[13] A medicinal chemistry effort focused on the amide scaffold led to the discovery of **2**; however, this scaffold was significantly less potent as a GIRK1/2 channel activator, as compared to **1**, and it was equipotent as an activator against the GIRK1/4 channel.[13] Mining this previous data led us to postulate that it may be possible to merge these two scaffolds – utilizing the pyrazole 'privileged scaffold' from the urea scaffold with the phenylacetamide portion of **2** to develop novel amide compounds that may allow for improved brain penetration as well as improved selectivity for GIRK1/4 (selectivity criteria of >10-30-fold). The results of this effort are presented below.

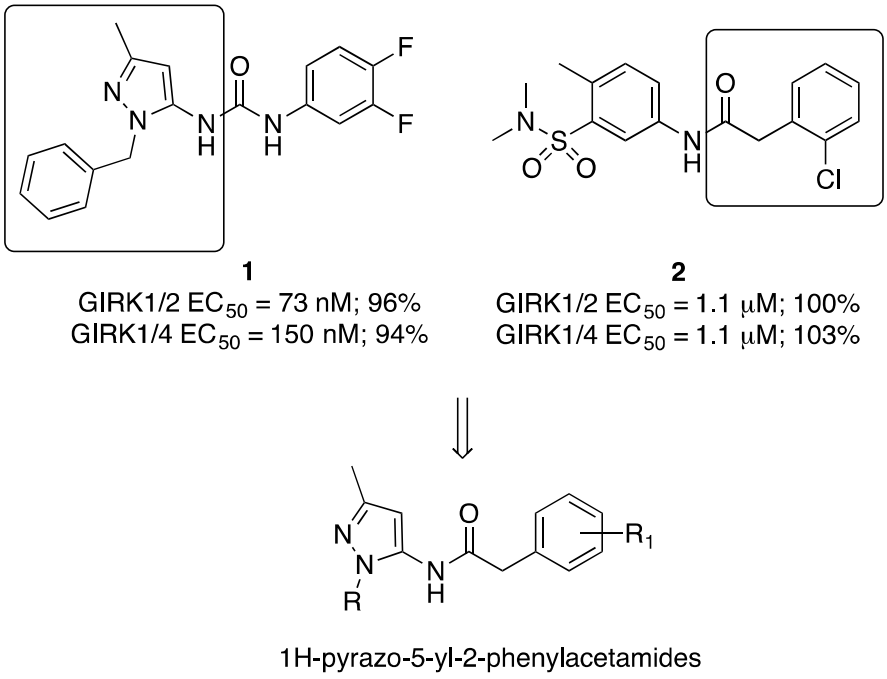

Figure 1. Structures of the previously reported GIRK1/2 activators and the merged pyrazol-5-ylphenylacetamides.

RESULTS AND DISCUSSION

The synthesis of the pyrazol-5-ylphenylacetamide analogs is outlined in Scheme 1. The appropriately substituted hydrazine, **3**, was reacted with 3-aminobut-2-enenitrile, **4**, under acidic conditions to generate the substituted aminopyrazoles, **5** in modest yield.[14] The final compounds (**7** – **10**) were obtained by PyClU amide coupling of the acid[15], **6**, with the newly formed (or commercially available) aminopyrazoles, **5**.

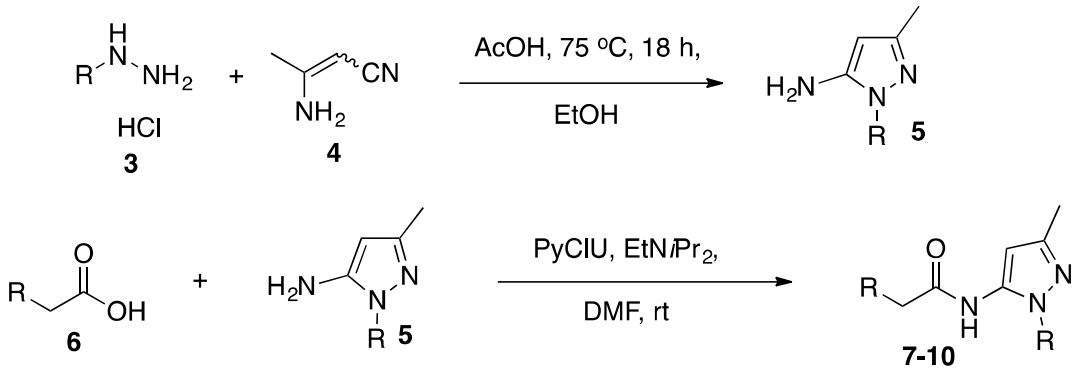

Scheme 1. Synthesis of the pyrazol-5-ylphenylacetamide analogs.

The initial SAR library focused on maintaining the substituent on the pyrazole constant (benzyl) and evaluating a variety of acetamides to test whether these were viable replacements of the urea moiety (Table 1). The initial 3,4-difluoro comparator, **7a**, was tested and was shown to lose significant activity compared to the urea analog, **1** (EC_{50} = 1.97 μM vs. EC_{50} = 0.073 μM). Replacing the 3,4-difluorophenyl with a 3-chloro-4-fluorophenyl, **7b**, produced an ~4-fold increase in potency (EC_{50} = 0.478 μM); which is still ~5-fold less potent than the urea analog, but did improve upon the potency of the original amide scaffold (**2**, EC_{50} = 1.1 μM). However, **7b**, provided a slight improvement in the selectivity for GIRK1/2 versus GIRK1/4 channel subtypes (~4-fold

selectivity vs. ~2-fold selectivity for **1**). Unfortunately, other modifications of the phenyl portion did not lead to an improvement over **7b**. The unsubstituted phenyl derivative (**7c**, EC_{50} = >10 μM) lost significant activity and we were able to regain some of the activity with other substituents (4-bromo-3-fluoro, **7d**, EC_{50} = 1.35 μM; naphthyl, **7f**, EC_{50} = 1.05 μM; 3,4-dichloro, **7g**, EC_{50} = 1.45 μM), but none of these compounds produced a molecule as active as the urea analog, **1**.

Table 1. SAR evaluation of the initial pyrazol-5-ylphenylacetamides.

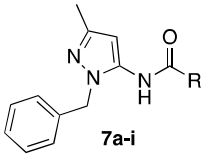

7a-i

Cmpd	R	GIRK1/2 (μM ± SEM[a]; % ± SEM[b])	GIRK1.4 (μM ± SEM[a]; % ± SEM[b])
1	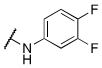	0.073 ± 0.007; 96.0 ± 1.1	0.150 ± 0.021; 94.0 ± 1.5
7a	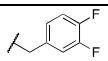	1.97 ± 0.33; 74.7 ± 7.8	3.98 ± 0.19; 46.0 ± 4.0
7b	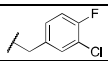	0.478 ± 0.077; 94.5 ± 5.5	2.0 ± 0.8; 100 ± 0
7c		>10; >25	>10; >15
7d	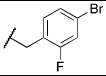	1.35 ± 0.17; 36.3 ± 4.9	2.75 ± 0.74; 17.0 ± 0.7
7e		inactive	inactive
7f	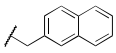	1.05 ± 0.14; 32 ± 1%	1.32 ± 0.22; 12.0 ± 0.3%
7g	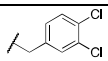	1.45 ± 0.35; 62.0 ± 5.5%	2.01 ± 0.41; 35.0 ± 3.0%
7h	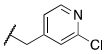	>6.9; >56%	>10; >42%
7i		inactive	inactive

[a] Potency values were obtained from triplicate determinations; values are average of n = 3. [b] Reported efficacy values shown are obtained from triplicate determinations; values are average of n = 3 and are normalized to a standard compound, **1**.

The next round of SAR evaluation was focused on the pyrazole *N*-substituent (Table 2). For this evaluation, we chose to hold the 3-chloro-4-fluorophenylacetamide constant in order to obtain a frame of reference for potency comparisons. Replacing the benzyl group with cyclohexyl, **8a**, proved to be a productive change as the potency increased ~3-fold over the *N*-benzylpyrazole analog (**8a**, EC_{50} = 0.165 μM vs. **7b**, EC_{50} = 0.478 μM). The potency was maintained after the insertion of a flexible methylene linker to form the cyclohexylmethyl substituent, **8b** (EC_{50} = 0.135 μM). These changes, although offering an improvement in GIRK1/2 channel potency, did not dramatically change the selectivity profile of the compounds. Eliminating the cyclohexyl ring and replacing with the *sec*-butyl group, **8c**, led to a loss of activity (EC_{50} = 0.536 μM); however, it was similar in potency to the original benzyl analog. Interestingly, addition of a heteroatom to moieties in this region of the molecule led to significant reduction in activity. Namely, addition of a nitrogen to the benzyl moiety (i.e., 4-pyridylmethyl, **8d**, EC_{50} >10 μM) led to an ~20-fold reduction compared to the benzyl counterpart; and addition of an oxygen to the cyclohexyl analog (i.e., 4-pyran, **8e**, EC_{50} = 3.07 μM) also led to an ~20-fold reduction in activity. Evaluation of additional alkyl (branched or unbranched, **8g-l**) led to the identification of other submicromolar compounds (**8j**, EC_{50} = 0.840 μM; **8k**, EC_{50} = 0.483 μM; **8l**, EC_{50} = 0.684 μM), signifying tolerance for flexible groups. However, none of these compounds improved upon the potency or selectivity compared to the cyclohexyl compounds. In addition, cycloalkyl groups were also investigated both directly attached to the pyrazole and those with a methylene spacer group. Contracting the ring system from a 6-membered ring to 3-, 4- or 5-membered rings was deleterious to the activity, with only the cyclopentyl group showing

midnanomolar activity (**8p**, EC_{50} = 0.518 μM). Lastly, direct branched alkyl groups (*t*-Bu, **8o**, inactive; *i*-Pr, **8q**, EC_{50} = 1.06 μM) were either inactive or showed significant loss of activity.

Table 2. Evaluation of the pyrazole *N*-substituent.

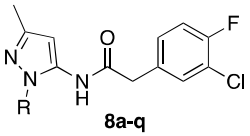

8a-q

Cmpd	Structure	GIRK1/2 (μM ± SEM; % ± SEM)	GIRK1.4 (μM ± SEM; % ± SEM)
8a		0.165 ± 0.012; 87.3 ± 0.9%	0.720 ± 0.213; 50.5 ± 5.5%
8b		0.135 ± 0.024; 82.0 ± 3.5%	0.534 ± 0.285; 52.3 ± 7.4%
8c		0.536 ± 0.093; 99.5 ± 3.5%	3.26 ± 0.44; 111 ± 4%
8d		>10; >42%	>10; >25%
8e		3.07 ± 0.79; 86.0 ± 5.6%	>10; >35%
8f		5.78 ± 1.52; 66.8 ± 6.8%	>10; >33%
8g		5.58 ± 0.66; 77.0 ± 11.4%	>10; >63%
8h		2.63 ± 0.73; 97.3 ± 10.4%	6.70 ± 1.68; 100.3 ± 10.0%
8i		1.40 ± 0.27; 89.7 ± 9.1%	5.93 ± 1.36; 80.0 ± 4.6%
8j		0.840 ± 0.180; 82.3 ± 5.8%	1.95 ± 0.52; 91.7 ± 8.4%
8k		0.483 ± 0.084; 57.3 ± 6.3%	1.49 ± 0.31; 55.3 ± 2.5%
8l		0.684 ± 0.072; 69.5 ± 5.3%	1.74 ± 0.13; 30.5 ± 8.5%
8m		>10; >34%	>10; >18%
8n		1.52 ± 0.41; 102.0 ± 5.5%	5.40 ± 1.34; 97.7 ± 6.8%
8o		inactive	inactive
8p		0.518 ± 0.091; 87.0 ± 7.3%	2.15 ± 0.56; 80.3 ± 8.5%
8q		1.06 ± 0.34; 101 ± 2%	8.50 ± 1.50; 67.5 ± 0.5%

[a] Potency values were obtained from triplicate determinations; values are average of n = 3. [b] Reported efficacy values shown

are obtained from triplicate determinations; values are average of n = 3 and are normalized to a standard compound, **1**.

In order to more fully explore the scope of the phenylacetamide substitution tolerance as well as other urea replacements, we synthesized a number of alternative analogs (Table 3). The branching of the methylene group of the phenylacetamide was explored with both quaternary center (cyclopropyl, **9a**) and (*R*)- and (*S*)-methyl substituents (**9b** and **9c**). Truncation of the phenylacetamide to the benzamide (**9c**) as well as reverse amide analogs (**9e** and **9f**), both with and without the methylene spacer, and finally squaramide derivatives as complete replacements were all examined. Unfortunately, none of these derivatives were active.

Table 3. SAR of substituted phenylacetamides, reverse amides and urea replacements.

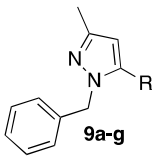

Cmpd	Structure	GIRK1/2 (μM ± SEM; % ± SEM)	GIRK1.4 (μM ± SEM; % ± SEM)
9a	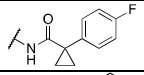	inactive	inactive
9b	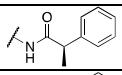	inactive	inactive
9c	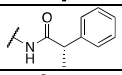	inactive	inactive
9d	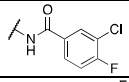	inactive	inactive
9e	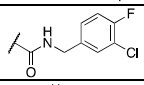	inactive	inactive
9f	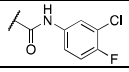	inactive	inactive

9g	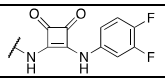	inactive	inactive

[a] Potency values were obtained from triplicate determinations; values are average of n = 3. [b] Reported efficacy values shown are obtained from triplicate determinations; values are average of n = 3 and are normalized to a standard compound, **1**.

Having established from the previous SAR evaluations that the cyclohexylmethyl and cyclohexyl substituents on the pyrazole were the most productive in terms of activity, we next more deeply investigated the SAR around the acetamide portion of the molecule (Table 4). As seen previously, the 3,4-difluorophenyl derivative, **10a**, was an active compound (EC_{50} = 0.149 μM) and was a significant improvement over the initial analog, **7a** (EC_{50} = 1.97 μM), and offered a slight improvement in selectivity (~5.7-fold selective over the GIRK1/4 subtype). Both the 2-chloro-4-fluoro, **10b** (EC_{50} = 0.343 μM), and 4-chloro-2-fluoro, **10c** (EC_{50} = 0.382 μM), derivatives were active, but were less active than the 3,4-substituted variants (**8b** or **10a**). This disparity in activity is also seen in the 2-fluoro-4-trifluormethoxy (**10d**, EC_{50} = 0.600 μM) versus the 4-fluoro-3-trifluoromethoxy analog (**10g**, EC_{50} = 0.245 μM). Further carbon substitutions were also tolerated with naphthalene (**10f**, EC_{50} = 0.405 μM) and 2-methylphenyl acetamide (**10i**, EC_{50} = 0.293 μM) having sub-500 nM activity.

Replacing the phenyl group with a variety of heterocyclic analogs was not as productive. The initial analog, 2-chloropyridine-4-yl acetamide, **10j**, retained most of the activity (EC_{50} = 0.396 μM); however, many of the other derivatives lost significant activity or were inactive. These include additional pyridine analogs (**10k-l**) and other 5-membered ring heteroaryl groups (**10m-o**) and indole derivatives (**10p-q**). Further replacement with cycloalkyl groups (indane, **10r**; difluorocyclopropyl, **10s**) were also not

productive analogs as they both lost activity. Lastly, a few analogs with the *N*-pyrazolecyclohexyl group were also evaluated (**10u-z**). As was seen previously, the cyclohexyl moiety produced compounds with similar range of potencies as the cyclohexylmethyl derivatives, and it was not obvious from the potency data that the cyclohexyl derivatives offered any advantages. However, the one analog where a dramatic increase in potency was observed was the 6-methylpyridin-3-yl acetamide, (**10w**, EC_{50} = 0.333 μM vs. **10k**, EC_{50} = >9.4 μM). Although the potency improvement was not obvious, a few cyclohexyl derivatives were more selective against GIRK1/4 (**10w**, 14-fold selectivity; **10x**, 12-fold selectivity; **10z**, inactive against GIRK1/4) than their previous counterparts.

Table 4. Further modification of phenylacetamide and *N*-pyrazole substituents.

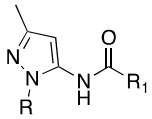

10a-z

Cmpd	R	R_1	GIRK1/2 (μM ± SEM; % ± SEM)	GIRK1.4 (μM ± SEM; % ± SEM)
10a		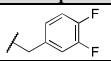	0.149 ± 0.009; 71.3 ± 2.6%	0.850 ± 0.475; 47.3 ± 7.5%
10b		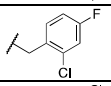	0.343 ± 0.127; 50.0 ± 4.6%	0.462 ± 0.019; 21.3 ± 3.3%
10c		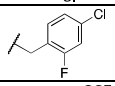	0.382 ± 0.165; 51.0 ± 2.3%	1.01 ± 0.05; 28.7 ± 4.7%
10d		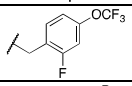	0.600 ± 0.201; 53.7 ± 2.9%	1.22 ± 0.03; 27.3 ± 3.7%
10e		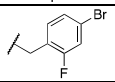	0.800 ± 0.130; 50.0 ± 5.0%	0.925 ± 0.220; 18.7 ± 2.8%
10f		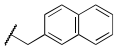	0.405 ± 0.105; 59.0 ± 5.6%	0.923 ± 0.162; 28.0 ± 5.3%
10g		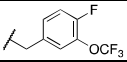	0.245 ± 0.063; 81.3 ± 4.4%	0.751 ± 0.142 65.3 ± 0.9%
10h		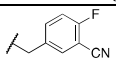	0.126 ± 0.013; 82.3 ± 3.5%	0.295 ± 0.071; 75.0 ± 3.6%

10i			0.293 ± 0.085; 44.0 ± 2.1%	0.930 ± 0.222; 29.7 ± 4.6%
10j		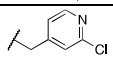	0.396 ± 0.029; 79.3 ± 2.0%	1.28 ± 0.02; 61.3 ± 4.7%
10k		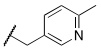	>9.4; >40%	inactive
10l			>10; >32%	inactive
10m			<10; >56%	>10; >21%
10n			2.38 ± 0.77; 61.7 ± 3.4%	<10; >21%
10o			0.892 ± 0.107; 59.5 ± 0.5%	2.59 ± 0.25; 28.0 ± 3.3%
10p		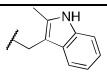	inactive	inactive
10q		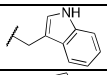	inactive	inactive
10r		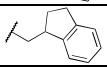	inactive	inactive
10s			1.10 ± 0.04; 25.5 ± 0.5%	inactive
10t		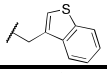	2.04 ± 0.74; 73 ± 21%	>10; >79%
10u		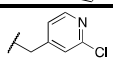	2.30 ± 0.02; 91.0 ± 7.3%	>10; >60%
10v		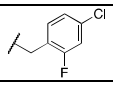	1.01 ± 0.30; 83 ± 12%	>10; >54%
10w		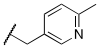	0.333 ± 0.023; 75 ± 0%	4.79 ± 2.78; 23.5 ± 4.5%
10x		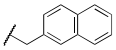	0.150 ± 0.020; 75.0 ± 2.5%	1.79 ± 1.07; 37.7 ± 1.9%
10y		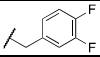	0.392 ± 0.072; 76.0 ± 7.5%	2.06 ± 0.42; 41.0 ± 2.5%
10z		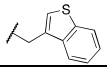	0.505 ± 0.175; 50.0 ± 9.5%	inactive

[a] Potency values were obtained from triplicate determinations; values are average of n = 3. [b] Reported efficacy values shown are obtained from triplicate determinations; values are average of n = 3 and are normalized to a standard compound, **1**.

Having identified a number of unique 1*H*-pyrazol-5-yl-2-phenylacetamide GIRK1/2 channel activators, we further profiled selected compounds in *in vitro* DMPK assays to assess their human and mouse liver microsomal intrinsic clearance and plasma protein binding. All but a few compounds evaluated displayed high intrinsic clearance and were predicted to have high hepatic clearance *in vivo* (CL_{HEP} > 75% Q_H).[16, 17] Both compounds **8e** and **8f** were predicted to have moderate clearance

(~<50% Q_H) in both human and mouse. Interestingly, both of these compounds were cycloheteroalkyl substituents (**8e**, 4-tetrahydropyran; **8f**, tetrahydrothiophene-1,1-dioxide). Using equilibrium dialysis, the plasma protein binding of the selected compounds was determined in human and mouse plasma.[18] The results revealed that the compounds had varying degrees of free fraction in human (F_u: 0.003 to 0.348) and mouse (F_u: 0.010 to 0.423) plasma; however, a number of compounds were unstable in mouse plasma. Interestingly, both **8e** and **8f** displayed the highest free fraction in human and mouse, and coupled with the predicted clearance these compounds possess the most attractive *in vitro* DMPK profile; unfortunately, these compounds are not very active as GIRK1/2 channel activators. However, these substituents may inform the next round of compound optimization. Further compounds for evaluation (**10f**–**10y**) all exhibited high clearance and many of these compounds were unstable in mouse plasma. Lastly, we evaluated a smaller set of selected compounds (**7b**, **8a**, **8c**) in a mouse IP cassette study in order to assess their ability to cross the blood-brain barrier (BBB).[19, 20] All of the compounds were brain penetrant with K_p values > 0.5 – 0.9. This represents a significant improvement over the previously reported urea scaffolds where many of those analogs had low brain distribution (K_p < 0.2).

Table 5. *In vitro* and *in vivo* DMPK properties of selected compounds.

Cmpd	GIRK1/2 (μM ± SEM)	Intrinsic Clearance (mL/min/kg)				Plasma Protein Binding (F_u)[b]	
		hCL_{INT}	hCL_{HEP}[a]	mCL_{INT}	mCL_{HEP}[a]	Human	Mouse
7b	0.478 ± 0.077	ND	ND	690	79.6	ND	0.071
8a	0.165 ± 0.012	246	19.3	622	78.6	0.009	0.136
8b	0.135 ± 0.024	1390	20.7	>5930	88.7	0.003	*
8c	0.536 ± 0.093	156	18.5	1070	83.0	0.016	0.172
8e	3.07 ± 0.79	23.6	11.1	85.7	43.9	0.211	0.423
8f	5.78 ± 1.52	14.3	8.50	18.0	15.0	0.348	0.362
8h	2.63 ± 0.73	47.7	14.6	657	79.2	0.054	0.171
10f	0.405 ± 0.105	2080	20.8	>5930	88.7	0.003	*

10g	0.245 ± 0.063	1900	20.7	>5930	88.7	0.002	0.010
10h	0.126 ± 0.013	648	20.3	2970	87.4	0.020	0.071
10t	2.04 ± 0.74	>2770	20.8	>5930	88.7	0.003	*
10w	0.333 ± 0.023	139	18.2	990	82.5	0.021	0.125
10x	0.150 ± 0.020	1020	20.6	>5930	88.7	0.013	*
10y	0.392 ± 0.072	92.5	17.1	2079	86.3	0.029	*

Mouse Cassette (IP, 0.25 mg/kg, 0.25 h)			
	Plasma (ng/mL)	**Brain (ng/g)**	K_p[c]
7b	101	63.4	0.61
8a	87.6	75.5	0.87
8c	190	104	0.55

[a]Predicted hepatic clearance based on intrinsic clearance in mouse and human liver microsomes using the well-stirred organ CL model (binding terms excluded). [b]F_u = fraction unbound. [c]K_p = total brain:plasma ratio. *unstable in mouse plasma.

CONCLUSION

In conclusion, we have identified a novel series of 1*H*-pyrazol-5-yl-2-phenylacetamides as brain-penetrant GIRK1/2 channel activators. The genesis of this series of compounds originated from a merging of two previously disclosed scaffolds that contained a urea moiety and an amide moiety. SAR around the pyrazole identified the cyclohexyl and cyclohexylmethyl groups as the optimal substituents. The acetamide portion allowed for more structural diversity, incorporating substituted phenyl and heteroaryl groups culminating in number of compounds with EC_{50}s between 100 and 200 nM. An improvement in the channel subtype selectivity profile was also seen for selected compounds; however, a universal improvement has not been realized at this point. Lastly, a number of compounds evaluated displayed moderate-high brain distribution (K_p = >0.5), which signifies an improvement over the previous GIRK1/2 channel activators that have been reported. Further *in vivo* evaluation of the lead molecules in models of anxiety is on-going and will be reported in due course.

METHODS

General. All NMR spectra were recorded on a 400 MHz AMX, AV-400 or Avance III HD 500 MHz Bruker NMR spectrometer. ^{1}H and ^{13}C chemical shifts are reported in δ values in ppm downfield with the deuterated solvent as the internal standard. Data are reported as follows: chemical shift, multiplicity (s = singlet, d = doublet, t = triplet, q = quartet, b = broad, m = multiplet), integration, coupling constant (Hz). Low resolution mass spectra were obtained on an Agilent 6120 or 6150 with ESI source. Method A: MS parameters were as follows: fragmentor: 70, capillary voltage: 3000 V, nebulizer pressure: 30 psig, drying gas flow: 13 L/min, drying gas temperature: 350 ^{o}C. Samples were introduced via an Agilent 1290 UHPLC comprised of a G4220A binary pump, G4226A ALS, G1316C TCC, and G4212A DAD with ULD flow cell. UV absorption was generally observed at 215 nm and 254 nm with a 4 nm bandwidth. Column: Waters Acquity BEH C18, 1.0 x 50 mm, 1.7 um. Gradient conditions: 5% to 95% CH_3CN in H_2O (0.1% TFA) over 1.4 min, hold at 95% CH3CN for 0.1 min, 0.5 mL/min, 55 ^{o}C. Method B: MS parameters were as follows: fragmentor: 100, capillary voltage: 3000 V, nebulizer pressure: 60 psig, drying gas flow: 12 L/min, drying gas temperature: 350 ^{o}C. Samples were introduced via an Agilent 1260 HPLC comprised of a degasser, G7111A quaternary pump, G4237A ALS, G7116A TCC, G1314 VWD with a ULD flow cell. UV absorption was generally observed at 215 nm and 254 nm with a 4 nm bandwidth. Column: Poroshell 120, SB-C18, 4.6 x 75 mm, 2.7 mm. Gradient conditions: 5% to 80% CH_3CN in H_2O (0.1% TFA) from 0 – 4 min, 80 to 95% CH_3CN in H_2O (0.1% TFA) from 4 – 6 min, hold at 95% CH_3CN from 6 – 8 min, 95% CH_3CN for 0.1 min, 1.5 mL/min, 45 ^{o}C. High resolution mass spectra were obtained on a Waters Micromass® Q-TOF with ESI source. Solvents for extraction,

washing and chromatography were HPLC grade. All reagents were purchased from commercial sources and were used without purification.

Materials and Methods for *in vitro* Pharmacology

Thallium flux assays were preformed essentially as previously described (Kaufmann et al). Briefly, HEK-293 cells expressing either GIRK1 and GIRK2 or GIRK1 and GIRK4 were cultured in α-MEM (Corning, Corning, NY) containing 10% (v/v) fetal bovine serum (Thermo Fisher Scientific, Waltham, MA) plus 1x glutagro (Corning, Corning, NY) (referred to hereafter as cell culture medium) at 37 C^o in a humidified 5% CO_2 atmosphere. Cells at ~90% confluence were dislodged from the tissue culture vessel using TrypLE Express (Thermo Fisher Scientific, Waltham, MA) and plated at a density of 20,000 cells/well in 20 μL/well cell culture medium in 384-well, clear-bottom, black-walled, BD PureCoat Amine plates (Corning, Corning, NY) and incubated over night at 37° C in a humidified 5% CO_2 atmosphere. On the day of assay the medium was removed from the plates and replaced with 20 μL/well of a solution containing assay buffer (Hanks Buffered Saline Solution (Thermo Fisher Scientific, Waltham, MA) plus 10 mM HEPES (Thermo Fisher Scientific, Waltham, MA)-NaOH, pH 7.2), 1 μM Thallos (TEFlabs, Austin, TX), 0.5% DMSO and 0.036% Pluronic F-127 (Sigma-Aldrich, St. Louis, MO). Cell plates containing Thallos solution were incubated 1 h at room temperature. Following incubation the Thallos-containing solution was replaced with 20 μL/well assay buffer. The Thallos-loaded cell plates were transferred to a Panoptic kinetic imaging plate reader (WaveFront Biosciences, Franklin, TN). Images acquired at 1 Hz, 480/40 nm excitation and 538/40 nm emission were collected for 10 s after which time 20 μL/well of assay buffer containing test compounds at 2-fold over their final

concentrations were added. Imaging continued for 4 min at which time 10 μL/well of a solution containing 125 mM $NaHCO_3$, 1.8 mM $CaSO_4$, 1 mM $MgSO_4$, 5 mM glucose, and 2 mM Tl_2SO_4, 10 mM HEPES-NaOH pH 7.2 was added and images were collected for an additional 2 min. To quantify test compound effects on GIRK channel activity, the initial slopes of the thallium-evoked changes in fluorescence were fit to a 4-parameter logistic equation using the Excel (Microsoft, Redmond, WA) plugin XLfit (IDBS, Guildford, UK) to obtain potency and efficacy values. Efficacies are relative to a maximally effective concentration of **1**, our most potent and effective activator which shows low selectivity between GIRK1/2 and GIRK1/4 channel subtypes. Ten-point concentration series from 30 μM to 1.5 nM were generated using an Echo liquid handler (Labcyte, San Jose, CA). Final DMSO concentration, 0.24% (v/v), in the assay was constant across all compound concentrations. Unless otherwise indicated, all buffer salts were obtained from Sigma-Aldrich, St. Louis, MO.

General Procedure for Amide Couplings. A one dram vial equipped with magnetic stir bar and screw cap vial was charged with the appropriate phenyl acetic acid, **6**, derivative (0.10 mmol), chlorodipyrrolidinocarbenium hexafluorophosphate (PyClU) (33 mg, 0.10 mmol), DMF (0.3 mL), Hunig's Base (0.1 mL, 0.57 mmol) and was stirred for approximately 5 minutes. The appropriate 5-Amino pyrazole, **5**, (0.10 mmol) was added and the reaction stirred until LCMS analysis indicated significant consumption of the starting materials (10 mins-18 hours). The crude reaction mixture was purified via mass-directed acidic reverse phase preparative HPLC to yield the corresponding amide products.

2-(3-cyano-4-fluorophenyl)-*N*-(1-(cyclohexylmethyl)-3-methyl-1*H*-pyrazol-5-yl)acetamide (10h): Following the general procedure above, compound (**10h**) was obtained (25.0 mg, 69%).

Analytical LCMS: R_T = 4.135 min; >95% @ 254 nm; MS (ESI^+) *m/z* 355.1 $[M + H]^+$.

^{1}H NMR (499 MHz, DMSO-d_6) δ 9.97 (s, 1H), 7.86 (dd, *J* = 6.3, 2.2 Hz, 1H), 7.74 (ddd, *J* = 8.0, 5.3, 2.3 Hz, 1H), 7.53 (t, *J* = 9.1 Hz, 1H), 5.96 (s, 1H), 3.74 (s, 2H), 3.66 (d, *J* = 7.2 Hz, 2H), 2.08 (s, 3H), 1.68 – 1.52 (m, 4H), 1.38 (d, *J* = 12.8 Hz, 2H), 1.07 (q, *J* = 9.7, 9.0 Hz, 3H), 0.84 – 0.69 (m, 2H). ^{13}C NMR (126 MHz, DMSO-d_6) δ 168.54, 145.98, 137.58, 137.50, 136.60, 134.65, 133.87, 133.85, 117.06, 116.91, 114.41, 100.34, 100.22, 98.95, 53.62, 41.12, 38.30, 30.32, 26.33, 25.61, 14.22. HRMS calc'd for $C_{20}H_{23}FN_4O$: 354.1856; found: 355.1934 $[M + H]^+$.

ASSOCIATED CONTENT

Supporting Information

The Supporting Information is available free of charge on the ACS Publications website at DOI:

Chemical synthesis of all analogs, *in vitro* Pharmacology procedures, *in vitro* PK methods, *in vivo* PK methods (PDF).

AUTHOR INFORMATION

Corresponding Author

*Phone: +1-402-559-9729. Fax: +1-402-559-5643. Email: corey.hopkins@unmc.edu

Author Contributions

C.R.H oversaw and designed the chemistry. J.M.W., A.K.V., and S.S. performed the synthetic chemistry work. T.M.B., J.S.D., and R.D.M. designed and performed the drug metabolism and pharmacokinetic *in vitro* experiments and *in vivo* studies. K.W. helped with the manuscript and in vivo studies. C.D.W. designed and analyzed the *in vitro* pharmacology experiments. K.K.A. performed and analyzed the *in vitro* pharmacology experiments. C.R.H. wrote the manuscript with input from all authors.

Funding

The work was supported by a NIH Grant 5R01MH107399 (C.R.H., C.D.W., and K.W.).

Notes

C.D.W. is the president of WaveFront Biosciences, the maker of the Panoptic kinetic imaging plate reader used to perform the *in vitro* pharmacology experiments. C.D.W. obtains royalties from the sale of Thallos thallium-sensitive fluorescent dye used for the *in vitro* pharmacology experiments. All other authors declare no competing financial interest.

ACKNOWLEDGMENTS

The authors would like to thank Sichen Chang and Xiaoyan Zhan for their contributions to the DMPK screening tier assays.

REFERENCES

(1) Lüscher, C. and Slesinger, P.A. (2010) Emerging roles for G protein-gated inwardly rectifying potassium (GIRK) channels in health and disease. *Nat. Rev. Neurosci. 11*, 301-315.

(2) Hibino, H., Inanobe, A., Furutani, K., Murakami, S., Findlay, I., and Kurachi, Y. (2010) Inwardly rectifying potassium channels: their structure, function, and physiological roles. *Physiol. Rev. 90*, 291-366.

(3) Lüscher, C. and Slesinger, P.A. (2010) Emerging roles for G protein-gated inwardly rectifying potassium (GIRK) channels in health and disease. *Nature Rev. Neuroscience 11*, 301-315.

(4) Kloukina, V., Herzer, S., Karlsson, N., Perez, M., Daraio, T., and Meister, B. (2012) G-protein-gated inwardly rectifying K+ channel 4 (GIRK4) immunoreactivity in chemically defined neurons of the hypothalmic arcuate nucleus that control body weight. *J. Chem. Neuroanat. 44*, 14-23.

(5) Luján, R., Marron Fernandez de Velasco, E., Aguado, C., and Wickman, K. (2014) New insights into the therapeutic potential of GIRK channels. *Trends Neurosci. 37*, 20-29.

(6) Kobayashi, T. and Ikeda, K. (2006) G protein-activated inwardly rectifying potassium channels as potential therapeutic targets. *Curr. Pharm. Des. 12*, 4513-4523.

(7) Walsh, K.B. (2011) Targeting GIRK channels for the development of new therapeutic agents. *Front. Pharmacol. 2*, 64.

(8) Niswender, C.M., Johnson, K.A., Luo, Q., Ayala, J.E., Kim, C., Conn, P.J., and Weaver, C.D. (2008) A novel assay of $G_{i/o}$-linked G protein-coupled receptor coupling to potassium channels provides new insights into the pharmacology of the group III metabotropic glutamate receptors. *Mol. Pharmacol. 73*, 1213-1224.

(9) Kaufmann, K., Romaine, I., Days, E., Pascual, C., Malik, A., Yang, L., Zou, B., Du, Y., Sliwoski, G., Morrison, R.D., Denton, J., Niswender, C.M., Daniels, J.S., Sulikowski, G.A., Xie, X., Lindsley, C.W., and Weaver, C.D. (2013) ML297 (VU0456810), the first potent and selective activator of the GIRK potassium channel, displays antiepileptic properties in mice. *ACS Chem. Neurosci. 4*, 1278-1286.

(10) Wydeven, N., Fernandez de Velasco, E.M., Du, Y., Benneyworth, M.A., Hearing, M.C., Fischer, R.A., THomas, M.J., Weaver, C.D., and Wickman, K. (2014) Mechanisms underlying the activation of G-protein–gated inwardly rectifying K^+ (GIRK) channels by the novel anxiolytic drug, ML297. *Proc. Natl. Acad. Sci. USA 111*, 10755-10760.

(11) Wen, W., Wu, W., Romaine, I., Kaufmann, K., Du, Y., Sulikowski, G.A., Weaver, C.D., and Lindsley, C.W. (2013) Discovery of 'molecular switches' within a GIRK activator scaffold that afford selective GIRK inhibitors. *Bioorg. Med. Chem. Lett. 23*, 4562-4566.

(12) Wen, W., Wu, W., Weaver, C.D., and Lindsley, C.W. (2014) Discovery of potent and selective GIRK1/2 modulators via 'molecular switches' within a series of 1-(3-cyclopropyl-1-phenyl-1*H*-pyrazol-5-yl)ureas. *Bioorg. Med. Chem. Lett. 24*, 5102-5106.

(13) Ramos-Hunter, S.J., Engers, D.W., Kaufmann, K., Du, Y., Lindsley, C.W., Weaver, C.D., and Sulikowski, G.A. (2013) Discovery and SAR of a novel series of GIRK1/2 and GIRK1/4 activators. *Bioorg. Med. Chem. Lett. 23*, 5195-5198.

(14) Sumesh, R.V., Muthu, M., Almansour, A.I., Kumar, R.S., Arumugam, N., Athimoolam, S., Prabha, E.A.J.Y., and Kumar, R.R. (2016) Multicomponent dipolar cycloaddition strategy: combinatorial synthesis of novel spiro-tethered pyrazolo[3,4-*b*]quinoline hybrid heterocycles. *ACS Comb. Sci. 18*, 262-270.

(15) Han, S.-Y. and Kim, Y.-A. (2004) Recent developments of peptide coupling reagents in organic synthesis. *Tetrahedron 60*, 2447-2467.

(16) Obach, R.S. (1999) Prediction of human clearance of twenty-nine drugs from hepatic microsomal intrinsic clearance data: an examination of in vitro half-life approach and nonspecific binding to microsomes. *Drug Metab. Disp. 27*, 1350-1359.

(17) Chang, G., Steyn, S.J., Umland, J.P., and Scott, D.O. (2010) Strategic Use of Plasma and Microsome Binding To Exploit in Vitro Clearance in Early Drug Discovery. *ACS Med. Chem. Lett. 1*, 50-63.

(18) Kalvass, J.C. and Maurer, T.S. (2002) Influence of nonspecific brain and plasma binding on CNS exposure: implications for rational drug discovery. *Biopharm. Drug Dispos. 23*, 327-338.

(19) Bridges, T.M., Morrison, R.D., Byers, F.W., Luo, S., and Daniels, J.S. (2014) Use of a novel rapid and resource-efficient cassette dosing approach to determine the pharmacokinetics and CNS distribution of small molecule 7-transmembrane receptor allosteric modulators in rat. *Pharmacol. Res. Perspect. 2*, e00077.

(20) Smith, N.F., Raynaud, F.I., and Workman, P. (2007) The application of cassette dosing for pharmacokinetic screening in small-molecule cancer drug discovery. *Mol. Cancer Ther. 6*, 428-440.

Table of Contents Graphic: